

See discussions, stats, and author profiles for this publication at: <https://www.researchgate.net/publication/231673244>

# Effect of Ozone Treatment on Surface Properties of Activated Carbon

ARTICLE *in* LANGMUIR · FEBRUARY 2002

Impact Factor: 4.46 · DOI: 10.1021/la010920a

---

CITATIONS

206

---

READS

285

4 AUTHORS, INCLUDING:



Hector Valdes

Catholic University of the Most Holy Concepti...

39 PUBLICATIONS 526 CITATIONS

SEE PROFILE



J. Rivera-Utrilla

University of Granada

186 PUBLICATIONS 6,068 CITATIONS

SEE PROFILE

# Effect of Ozone Treatment on Surface Properties of Activated Carbon

H. Valdés,<sup>\*,†</sup> M. Sánchez-Polo,<sup>‡</sup> J. Rivera-Utrilla,<sup>‡</sup> and C. A. Zaror<sup>†</sup>

*Departamento de Ingeniería Química (F. Ingeniería), Universidad de Concepción, Correo 3, Casilla 160-C, Concepción, Chile, and Departamento de Química Inorgánica (F. Ciencias), 18071-Universidad de Granada, Spain*

Received June 18, 2001

The combined use of ozone and activated carbon has recently started to be developed for the treatment of toxic effluents. However, the effect of ozone on the properties of activated carbon is not fully elucidated. A study was undertaken of modifications in the surface properties of a commercial activated carbon produced by its ozonation during different time periods. Surface chemistry of the activated carbon samples was characterized by selective neutralization, temperature-programmed desorption, X-ray photoelectron spectroscopy, and pH of the point of zero charge. Surface area and volume of micropores and mesopores were obtained from nitrogen adsorption isotherms at 77 K. Adsorption properties were determined by methylene blue adsorption index. Results show that the higher the ozone dose, the higher is the oxidation of the carbon and the greater is the number of acid groups present on the carbon surface, especially carboxylic groups, whereas the pH of the point of zero charge decreases. The surface area, micropore volume, and methylene blue adsorption all reduce with higher doses. These results are explained by the ozone attack on the carbon and the fixation of oxygen groups on its surface.

## 1. Introduction

Activated carbon has been widely used as a powerful adsorbent in wastewater and gases treatment. The chemical reactivity of the activated carbon surface has recently been emphasized, because it has been demonstrated to catalyze oxidation, reduction, halogenation, dehydrogenation, polymerization, and nucleophilic reactions, among others.<sup>1–5</sup> Activated carbon reactivity is directly related to its chemical properties, and the chemical reactivity with organic substrates can be attributed to the presence of carboxylic groups, hydroquinone free radicals, quinones, metallic ions, and nitrogenous impurities.<sup>1</sup>

Recently, the combined use of ozone and activated carbon in single treatment processes has been proposed as an attractive option for the destruction of toxic organic compounds.<sup>4,6,7</sup> The great oxidation power of ozone together with the high adsorption capacity of activated carbon effectively eliminates organic contaminants of high toxicity and low biodegradability<sup>7</sup> and prevents their mutagenic activity.<sup>8</sup>

Combined ozone–activated carbon treatment processes have been shown to modify the chemical composition of activated carbon surface groups.<sup>9,10</sup> These reactions may determine the adsorption capacity of the activated carbon,

its regeneration efficiency, and the process economic feasibility. Thus, greater knowledge of the surface chemistry of activated carbon could lead to the development of more specific and effective adsorbents for a given process.

The purpose of this study was to investigate modifications in both the surface chemistry and textural characteristics of activated carbon caused by the action of ozone. This work is part of a wider ongoing project to investigate the possibilities of the combined use of ozone and activated carbon in the elimination of contaminants from water.

## 2. Experimental Section

**2.1. Carbon Treatment.** Filtrasorb 400 (Calgon Carbon Corp.), a commercial activated carbon of bituminous origin, was used, denominated “F”, with particle size of 500–800  $\mu\text{m}$ . The carbon was washed with deionized water, oven-dried at 170 °C for 24 h, and stored in a desiccator until its use. The activated carbon was treated with ozone in a fixed bed reactor loaded with 2 g of carbon under a constant ozone flow of 76 mg of  $\text{O}_3/\text{min}$ , operating at 25 °C and 1 atm. Ozone was produced in an Ozovac ozone generator and fed to the reactor for different exposure times (10, 20, 30, 60, and 120 min). Inlet and outlet ozone was monitored by UV spectrophotometry (Spectronic Genesis 5) with a gas flow cell at 253.7 nm. After each treatment time, the carbon was withdrawn from the reactor and oven-dried, following a thermal program that allowed drying for 1 h at 60 °C, 1 h at 100 °C, 1 h at 150 °C, and 24 h at 170 °C. Dried samples were stored in a desiccator until use. Each treated sample was assayed for chemical and physical characterization. The  $\text{O}_3$ -treated carbon samples were denominated “F” followed by the number of minutes of the treatment.

**2.2. Chemical Characterization. 2.2.1. Surface Functional Group Determination.** Selective Neutralization Analysis. Acid and basic functional groups of the activated carbon surface were determined by the method proposed by Boehm.<sup>11</sup> Solutions of  $\text{NaHCO}_3$  (0.02 N),  $\text{Na}_2\text{CO}_3$  (0.02 N),  $\text{NaOH}$  (0.02 and 0.1 N), and  $\text{HCl}$  (0.02 N) were prepared using deionized

\* To whom correspondence should be addressed: Fax: 56-41-247491. E-mail: hvaldez@diq.udec.cl.

<sup>†</sup> Universidad de Concepción.

<sup>‡</sup> Universidad de Granada.

(1) Chen, C. C.; Lin, C. E. *Anal. Chim. Acta* **1996**, 321, 215–218.

(2) Juntgen, H.; Kuhl, H. In *Chemistry and Physics of Carbon*; Thrower, P. A., Ed.; Marcel Dekker: New York, 1989; Vol. 22, p 145.

(3) Bansal, R. C.; Donnet, J. B.; Stoeckli, F. *Active Carbon*; Marcel Dekker: New York, 1988.

(4) Cooney, D. O.; Zhenpeng, X. *AIChE J.* **1994**, 40 (2), 361–364.

(5) Marsh, H. *Introduction to Carbon Science*; Butterworth: London, 1989.

(6) McKay, G.; McAleavey, G. *Chem. Eng. Res. Des.* **1988**, 66, 532–536.

(7) Zaror, C. A. *J. Chem. Technol. Biotechnol.* **1997**, 70, 21–28.

(8) Mondaca, M. A.; Carrasco, V.; Zaror, C. A. *Bull. Environ. Contam. Toxicol.* **2000**, 64, 59–65.

(9) Sutherland, I.; Sheng, E.; Braley, R. H.; Freakley, P. K. *J. Mater. Sci.* **1996**, 31, 5651–5655.

(10) Zaror, C. A.; Soto, G.; Valdés, H.; Mansilla, H. *Wat. Sci. Technol.* **2001**, 44, 125–130.

(11) Boehm, H. P. *Adv. Catal.* **1966**, 16, 179–274.

**Table 1. Analysis of Ash Elements (%) by X-ray Fluorescence**

Si	Ti	Al	Fe	Mn	Mg	Ca	Na	K	P
20.19	0.82	8.41	6.32	0.02	0.49	1.79	0.31	0.55	0.02

water. A 20 mL volume of these solutions was added to vials containing 200 mg of activated carbon. These samples were shaken until equilibrium. In parallel, five blanks were prepared without carbon. When equilibrium was reached, the carbon was separated from the solution by decanting. The excess of base or acid was determined by back-titration, using hydrochloric acid (0.02 and 0.1 N) and sodium hydroxide (0.02 N) solutions.

**Temperature-Programmed Desorption (TPD).** These experiments were carried out by heating the samples in an He flow to 1273 K at a heating rate of 50 K/min and monitoring the amounts of CO and CO<sub>2</sub> with a mass spectrometer (Thermocube, Balzers Ltd), as described elsewhere.<sup>12</sup>

**X-ray Photoelectron Spectroscopy (XPS).** XPS spectra were obtained with a VG ESCALAB 220i-XL spectrometer, using an unmonochromatized Al K $\alpha$  X-ray source (1486.6 eV). The vacuum in the analysis chamber was under  $4 \times 10^{-9}$  mbar. The survey scan spectra were collected with a pass energy of 50 eV, whereas the high-energy resolution spectra were performed with the pass energy of 25 eV.

**2.2.2. Ash Analysis.** Total ash content was determined by incineration of the carbon. Components of the ashes were analyzed by X-ray fluorescence. The ash content of the carbon was 6.6% (d.b.). Data on the different elements detected in the ashes are listed in Table 1.

**2.2.3. pH of Point of Zero Charge (pH<sub>PZC</sub>).** pH<sub>PZC</sub> was determined using the mass titration method described by Noh and Schwarz.<sup>13</sup> NaNO<sub>3</sub> (0.01 M) solutions of pH 3, 6, and 11 were prepared using HNO<sub>3</sub> (0.1 M) and NaOH (0.1 M). A 100 mL volume solution of different initial pH and increasing amounts of carbon sample (0.1%, 0.5%, 1.1%, 5%, 10%, 15%, 20%) was added to 250 mL Erlenmeyer flasks. The equilibrium pH was measured after 24 h of shaking at  $25 \pm 0.1$  °C.

**2.3. Textural Characterization. Surface Area and Pore Volumes.** The surface area of the carbon samples and the volume of micropores and mesopores were obtained by N<sub>2</sub> adsorption at 77 K, using a Micromeritics Gemini 2370 sorptometer. For these experiments, 200 mg of sample was used, previously degassed at 350 °C for 3 h under nitrogen flow. The surface area data ( $S_{N_2}$ ) were calculated from the nitrogen adsorption data using the BET equation. Micropore ( $V_{mi}$ ) and mesopore ( $V_{me}$ ) volumes and the external surface area ( $S_{ext}$ ) were calculated by applying the  $\alpha$ -method to the N<sub>2</sub> adsorption data.<sup>14,15</sup>  $S_{ext}$  is the surface area corresponding to mesopores and macropores.

**2.4. Adsorptive Properties.** The adsorption capacity of the samples was evaluated by means of methylene blue adsorption, using the method described by Barton.<sup>16</sup> A 100 mg amount of the carbon samples was added to 50 mL vials with 25 mL of methylene blue at a concentration of 1200 mg/L in 5% acetic acid solution. In parallel, a blank was prepared with the methylene blue solution without carbon. The vials were shaken for 24 h at 25 °C. The concentration of methylene blue was determined spectrophotometrically.

### 3. Results and Discussion

**3.1. Surface Chemical Properties. 3.1.1. Surface Functional Groups. Selective Neutralization Analysis.** According to Boehm,<sup>11</sup> NaHCO<sub>3</sub> neutralizes carboxylic acids, Na<sub>2</sub>CO<sub>3</sub> neutralizes carboxylic and lactone groups, and NaOH neutralizes carboxylic, lactone, and phenol groups. Carbonyl groups are determined by the difference between the amount of 0.1 and 0.02 N NaOH consumed by the carbon. It is also established that neutralization

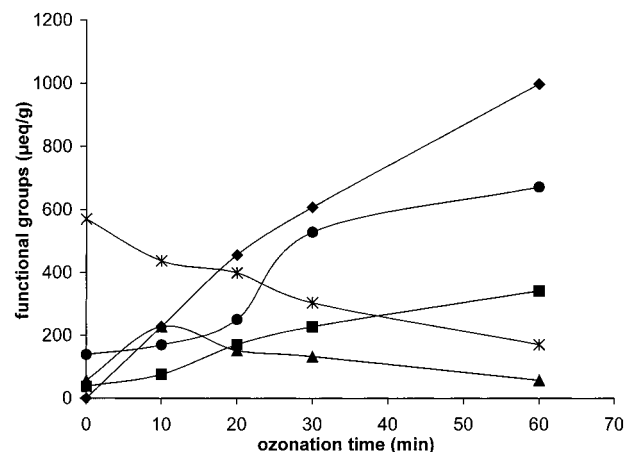


**Figure 1.** Variation in content of surface functional groups of activated carbon with ozone treatment: basic groups, \*; carboxylic groups, ♦; lactone groups, ■; phenol groups, ▲; carbonyl groups, ●.

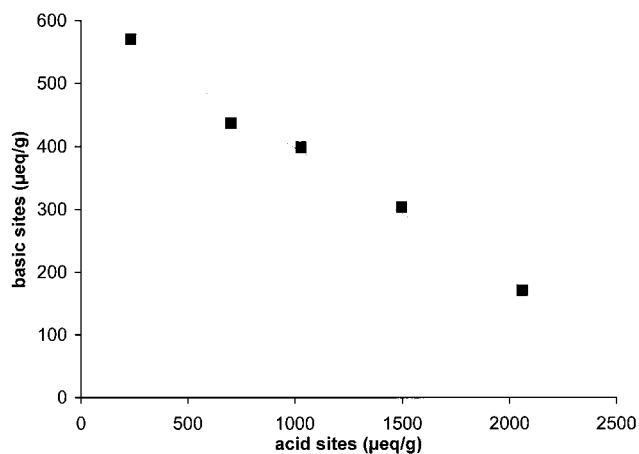


**Figure 2.** Variation in content of acid and basic sites during ozonation of activated carbon.

by HC1 reveals the amount of basic surface groups. Figure 1 shows the effect of ozone on the content of acid and basic surface functional groups. Clearly, the distribution of chemical groups on the carbon surface is significantly affected by the extent of ozonation. Indeed, the content of phenol groups decreases with ozonation time, generating more oxidized groups such as lactones and carbonyl and carboxylic groups. The latter presents a greater concentration as ozone exposure increases.

Moreover, the amount of acid sites on the activated carbon drastically increases with ozonation. Figure 2 shows a linear correlation ( $R^2 = 0.99$ ) between the concentrations of basic and acid sites in the different carbon samples, clearly demonstrating that the increase in acid sites is accompanied by a decrease in basic sites. Approximately five acid sites are formed for each basic site that disappears. Chromene and  $\gamma$ -pyrone type structures are reported to be responsible for the basic character of activated carbons.<sup>17</sup> On the other hand, the basic nature of activated carbon surface has also been related to the presence of delocalized  $\pi$  electrons on the basal plane of the surface of activated carbon.<sup>18</sup>

(12) Ferro-García, M. A.; Utrera-Hidalgo, E.; Rivera-Utrilla, J.; Moreno-Castilla, C.; Joly, J. P. *Carbon* **1993**, *31*, 857–863.

(13) Noh, J. S.; Schwarz, J. A. *Carbon* **1990**, *28*, 675–682.

(14) Gregg, S. J.; Sing, S. W. *Adsorption, Surface Area and Porosity*, 2nd ed.; Academic Press: London, 1982; Chapter 4.

(15) Rodríguez-Reinoso, F.; Martín-Martínez, J. M.; Prado-Burguete, C.; McEnaney, B. J. *J. Phys. Chem.* **1987**, *91*, 515–516.

(16) Barton, S. S. *Carbon* **1987**, *25*, 343–350.

(17) Boehm, H. P. *Carbon* **1994**, *32*, 759–769.

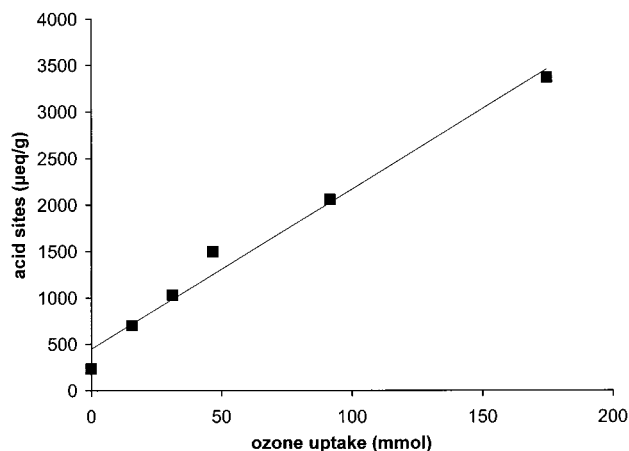


**Figure 3.** Amount of acid sites generated on activated carbon according to ozone consumption.

**Table 2.** Amounts of CO and CO<sub>2</sub> (μmol/g) Evolved in the TPD Analysis

sample	CO	CO <sub>2</sub>	CO/CO <sub>2</sub>	oxygen <sup>a</sup> (%)
F	790	170	4.64	1.82
F-10	1520	580	2.62	4.30
F-20	2470	1300	1.90	8.11
F-30	2850	1520	1.88	9.44
F-60	4160	2470	1.68	14.54
F-120	5300	5130	1.03	24.90

<sup>a</sup> From the amounts of CO and CO<sub>2</sub> evolved.

Figure 3 relates the ozone consumption to the amount of acid sites formed during the treatment time. The linear fit ( $R^2 = 0.989$ ) indicates that for each 1 mmol of ozone consumed, approximately 16 μequiv of acid sites are generated/g of activated carbon. The mechanism of the interaction of ozone and activated carbon has been reported to be similar that of ozone and alkenes.<sup>19</sup> In a first stage, the ozone is added to the double bond, forming an unstable intermediate, denominated primary ozonide. This primary ozonide then passes to the secondary ozonide (denominated molonozone), which is much more stable. Oxygenated groups are generated in the rupture of the secondary ozonide.<sup>19</sup> This mechanism explains the increase in the content of acid sites on the carbon surface. As can be seen in Figure 2, a fraction of the acid sites is formed through the oxidation of basic groups in the original carbon. Nevertheless, the generation of acid groups is mainly related to the addition of ozone to the double bonds of the carbon structure.

**TPD Analysis.** It is known that when carbonaceous material is subjected to a program of increasing temperature, the surface oxygen complexes desorb primarily as CO<sub>2</sub> and CO.<sup>3,5,20–23</sup> The CO<sub>2</sub> comes from the decomposition of carboxyl, anhydride, and lactone groups, and the CO from the decomposition of phenol, carbonyl, anhydride, pyrone, quinone, and ether groups.

TPD experiments were performed on all of the carbon samples. Table 2 lists the amounts of CO and CO<sub>2</sub> detected when they were heated to 1273 K and also shows the

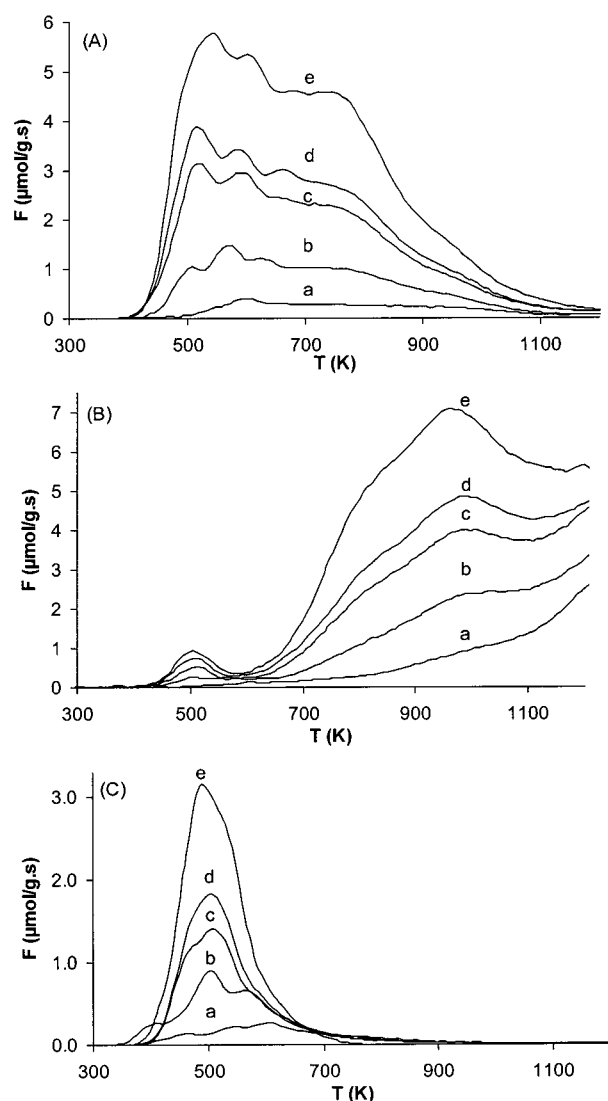


**Figure 4.** Thermal desorption of CO<sub>2</sub> (A), CO (B), and H<sub>2</sub>O (C) for F (a), F-10 (b), F-20 (c), F-30 (d), and F-60 (e).

percentage of oxygen of the samples obtained from the amounts of CO and CO<sub>2</sub> desorbed. The CO<sub>2</sub>, CO, and H<sub>2</sub>O desorption profiles of the samples are depicted in Figure 4.

The data listed in Table 2 indicate that when the carbon is ozonated, its oxygen content increases proportionately to the treatment time. The value of the CO/CO<sub>2</sub> ratio markedly decreases with longer ozone exposure times. These values indicate that O<sub>3</sub> treatment creates oxygen groups on the carbon surface that generate CO and CO<sub>2</sub> when they decompose and that more groups are formed that generate CO<sub>2</sub> (carboxylics and lactones) than those that generate CO. These results are consistent with the findings from selective titrations of the samples (Figure 1).

The CO<sub>2</sub> desorption profile of the original carbon (Figure 4a) indicates that the maximum evolution rate of this compound takes place at 595 K and shows a tail that extends to 1100 K. This profile suggests the presence of different groups and/or the same oxygen complex located in energetically different positions. The data shown in Figure 1 may indicate that the peak at 595 K is due to the presence of lactones.<sup>24</sup> In the CO profile of the original

(18) Leon y Leon, C. A.; Solar, J. M.; Calemma, V.; Radovic, L. *R. Carbon* **1992**, *30*, 797–811.

(19) Deitz, V. R.; Bitner, J. L. *Carbon* **1973**, *11*, 393–401.

(20) Mattson, J. S.; Mark, H. B. *Activated Carbon: Surface Chemistry and Adsorption from Solution*; Marcel Dekker: New York, 1971.

(21) Yoshinobu, O.; Jenkins, R. G. *Carbon* **1993**, *31*, 109–121.

(22) Moreno-Castilla, C.; Ferro-García, M. A.; Joly, J. P.; Bautista-Toledo, I.; Carrasco-Marín, F.; Rivera-Utrilla, J. *Langmuir* **1995**, *11*, 4386–4392.

(23) Figueiredo, J. L.; Pereira, M. F. R.; Freitas, M. M. A.; Orfao J. M. *Carbon* **1999**, *37*, 1379–1389.

(24) Marchon, B.; Carrazza, J.; Heinemann, H.; Somorjai, G. A. *Carbon* **1988**, *26*, 507–514.



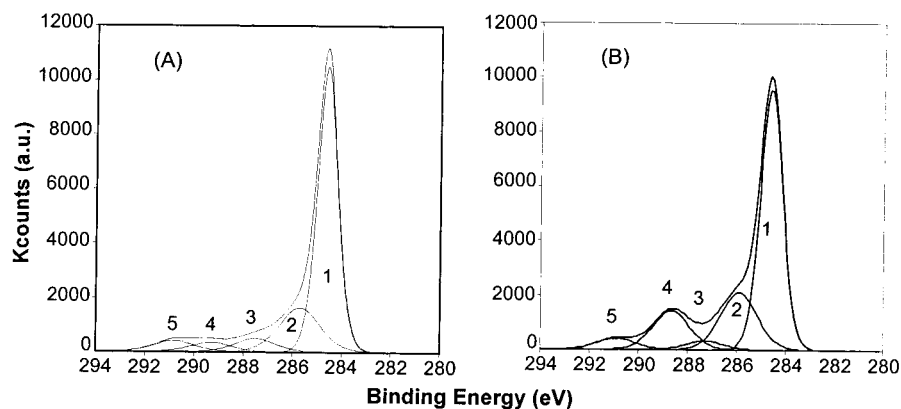


**Figure 5.** X-ray photoelectron spectra showing the C 1s core level in activated carbon for samples F (A) and F-60 (B): graphitic/aromatic or aliphatic (1); carbon in C–OH and C–O–C groups (2); carbon in C=O (3); carbon in COOH and COO–R (4);  $\pi$ – $\pi^*$  transitions in aromatics (5).

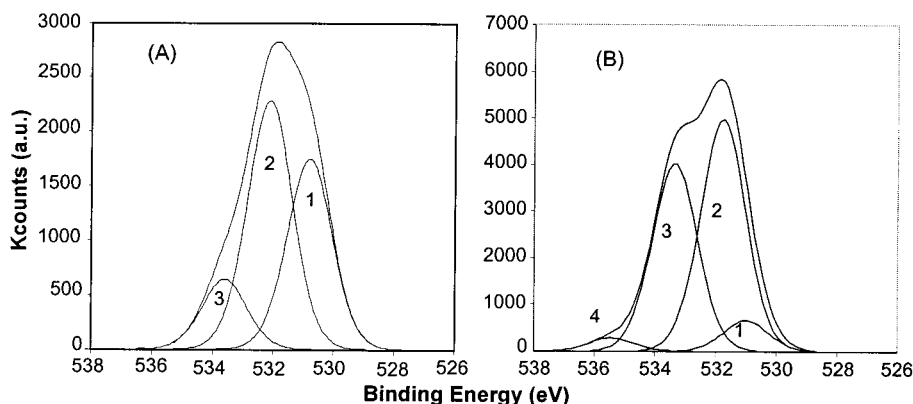


**Figure 6.** X-ray photoelectron spectra showing O 1s core level in activated carbon for samples F (A) and F-60 (B): oxygen in C=O groups (1); oxygen atoms in hydroxyl or ethers (2); oxygen in anhydride, lactone, carboxylic acids (3); chemisorbed  $O_2$ , water (4).

carbon (F), a maximum also appears at elevated temperatures (1200 K), which may be due to the presence of carbonyl groups<sup>25</sup> and/or to the decomposition of the pyrone group.<sup>26</sup> This group would be partly responsible for the highly basic nature of this carbon. The shoulder that appears at around 950 K is due to the presence of phenol groups.<sup>25</sup>

The  $CO_2$  and CO profiles of the ozone-treated carbon sample show a gradual increase in the size of the peaks that already appeared in the original carbon. Moreover, new peaks appear in the  $CO_2$  curve at low temperatures (515–640 K), which may be accounted for by the formation of strong carboxylic groups and lactone groups. A new peak is also detected in the CO profile at low temperatures (450–600 K), related to the generation of anhydride groups by condensation of two adjacent carboxylic groups when the sample is heated;<sup>27</sup> this process is confirmed by the presence of water at 450 K.

As the ozone treatment time increases, a progressive increase can be observed in the size of the peaks of  $CO_2$  that appear at low temperatures, because of an increased content of carboxylic and lactone groups in the carbon. An increased content of highly stable groups that decompose at elevated temperatures can also be seen, confirming the formation of carboxylic anhydrides.

**XPS Analyses.** The XPS spectra of both treated and untreated samples present two distinct peaks, due to carbon (C 1s) and oxygen (O 1s), as shown in Figures 5

and 6. The C 1s spectra have been resolved into five individual component peaks, as illustrated in Figure 5, namely the following: (1) graphitic, aromatic, or aliphatic carbon; (2) ether or phenol groups; (3) carbonyl groups; (4) carboxyl or esters groups; (5) shake-up satellite peaks due to a  $\pi$ – $\pi^*$  transitions in aromatic rings.<sup>25,28</sup>

On the other hand, as illustrated in Figure 6, the high-resolution O 1s spectra show the presence of 4 peaks: (1) oxygen in carbonyl groups (C=O); (2) oxygen atoms in hydroxyl or ethers; (3) oxygen in anhydride, lactone, or carboxylic acids; (4) chemisorbed oxygen or water.<sup>23</sup>

XPS results are summarized in Table 3. It is interesting to note that the surface oxygen fraction increases from about 14% to more than 24% due to ozonation. Moreover, the O 1s:C 1s ratio, which indicates the degree of surface oxidation, increases from 0.16 to 0.34 after ozonation. Lactone, anhydride, and carboxylic acid surface concentrations increase due to ozonation, whereas carbon in graphitic or aromatic surface structures is significantly reduced as a result of the increase in the oxidation level. These results confirm those obtained by TPD and selective neutralization.

**3.1.2. pH of the Point of Zero Charge ( $pH_{PZC}$ ).** Figure 7 depicts the  $pH_{PZC}$  for the F and F-60 samples as determined by mass titration, by way of illustration. The  $pH_{PZC}$  for each sample is obtained from the asymptotic value that the pH reaches when the mass fraction of the carbon is increased for different initial pH values. Figure 8 summarizes the variation in  $pH_{PZC}$  with increasing ozone

(25) Zielke, U.; Huttinger, J.; Hoffman, W. P. *Carbon* **1996**, *34*, 983–998.

(26) Fritz, O. W.; Huttinger, J. *Carbon* **1993**, *31*, 923–930.

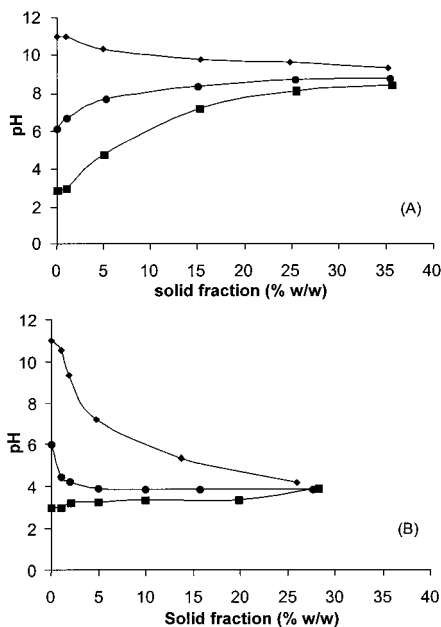
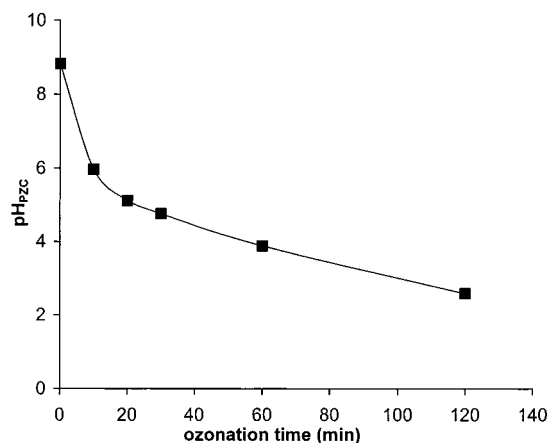
(27) Otake, Y.; Jenkins, R. G. *Carbon* **1993**, *31*, 109–121.

(28) Biniak, S.; Szymanski, S.; Siedlewski, J.; Swiatkowski, A. *Carbon* **1997**, *35*, 1799–1810.

**Table 3. XPS Results: Surface Composition for Untreated and 60-min Ozonated Carbon**

element	peak	functional groups	binding energy (eV)	activated carbon (% atomic)	
				F	F-60
C1s	1	graphitic, aromatic (C–C)	284.6	52.28	41.57
C1s	2	C in hydroxyl, ethers (C–OH, C–O–C)	286.0	16.07	14.55
C1s	3	C in carbonyl (C=O)	287.3	5.03	2.29
C1s	4	C in COOR (R = H or alkyl)	288.6	3.58	10.27
C1s	5	$\pi$ – $\pi^*$ transitions in aromatic	291.0	3.95	3.03
O1s	1	carbonyl, quinone (C=O)	530.7	5.30	1.59
O1s	2	hydroxyl, ethers (C–OH, C–O–C)	532.1	6.96	12.15
O1s	3	anhydride, lactone, carboxylic acids	533.3	1.95	9.86
O1s	4	chemisorbed H <sub>2</sub> O or O <sub>2</sub>	535.3		0.67

treatment time. The value of the  $\text{pH}_{\text{PZC}}$  decreases approximately six units after 120 min of ozone exposure. In the first 10 min, the  $\text{pH}_{\text{PZC}}$  with an initial value of 8.8 falls to 6, reaching a value of 2 after 120 min of ozonation. These results indicate that the carbon increases its density of surface negative charge with increasing ozone treatment time. In fact, a treatment of 120 min increases the pH interval for which the carbon has negative charge from 8.8–14 to 2–14. These results are of great interest for the use of the carbon samples as adsorbents, because the ozone treatment of the carbon favors the adsorption on it of cationic species, such as most metallic species, due to the

**Figure 7.** Determination of  $\text{pH}_{\text{PZC}}$  for samples F (A) and F-60 (B).**Figure 8.** Variation in  $\text{pH}_{\text{PZC}}$  with ozonation time.**Table 4.  $\text{p}K_a$  Values Calculated for Highly Oxidized Activated Carbon Samples**

	F-30	F-60	F-120
$\text{p}K_a$	7.8	5.9	3.9

enhancement of adsorbent–adsorbate electrostatic interactions.

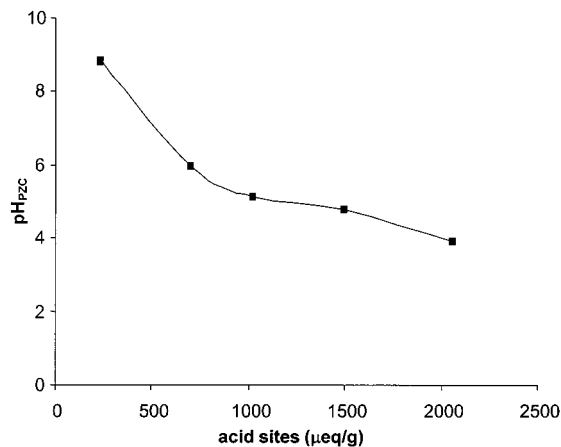
Figure 9 shows the relationship between the  $\text{pH}_{\text{PZC}}$  value and the concentration of acid sites on the carbon surface. The reduction in  $\text{pH}_{\text{PZC}}$  is related to the increase in acidic groups caused by the action of the ozone. The acid groups generated with the exposure of the activated carbon to ozone treatment, as deduced from the TPD, XPS, and selective neutralization experiments, would be the main cause of the development of the negative surface charge.

The degree of surface acidity of the ozone-treated activated carbon was obtained using the surface ionization method.<sup>29</sup> This model does not include the influence of the ash components. The ionization or acidity constant ( $K_a$ ) was determined for the highly oxidized carbon samples (F-30, F-60, and F-120), following the procedure described by Barton.<sup>30</sup> For this purpose, the results of the mass titration at an initial pH of 6 were used, and the basic sites content was considered to be negligible. The results are displayed in Table 4.

The ozone treatment reduces the  $\text{p}K_a$  of the activated carbon. Initially, the activated carbon has a basic character, but increasing exposure leads to the appearance of functions with greater acid strength. The value of  $\text{p}K_a$  calculated in this way is the overall result of the inductive effects of the oxygenated groups of the carbon surface. The average  $\text{p}K_a$  value of carbon ozonated for 120 min is within the range of values associated with keto acids (glyoxylic acid,  $\text{O}=\text{CHCOOH}$ ,  $\text{p}K_a = 3.34$ ).

### 3.2. Textural Characterization. Surface Area and Pore Volumes.

Table 5 lists the results for the surface

**Figure 9.** Relationship between  $\text{pH}_{\text{PZC}}$  and acid sites content of the carbon samples.

**Table 5. Textural and Adsorptive Properties of the Carbon Samples**

sample	$S_{N_2}$ (m <sup>2</sup> /g)	$V_{mic}$ (cm <sup>3</sup> /g)	$V_{me}$ (cm <sup>3</sup> /g)	$S_{ext}$ (m <sup>2</sup> /g)	$X_m(MB)$ (mg/g)	$S_{MB}$ (m <sup>2</sup> /g)
F	1000	0.474	0.019	53.7	98.8	328
F-10	1023	0.472	0.031	87.1	92.4	307
F-20	943	0.437	0.027	74.8	91.3	303
F-30	940	0.436	0.028	79.7	89.8	298
F-60	815	0.380	0.025	71.6	82.6	274
F-120	632	0.297	0.023	64.4	77.3	256

areas and volumes of micropores and mesopores obtained by quantitative analysis of nitrogen adsorption isotherms at 77 K in both the original and the ozone-treated activated carbon samples. A slight increase in surface area can be observed after 10 min of ozone exposure, followed by a gradual reduction as the time of exposure lengthens. The micropore volume shows a similar behavior. The volume of mesopores in this carbon is relatively low, increases slightly after 10 min of ozone exposure, and then remains constant in the remaining samples. The external surface area follows a similar behavior.

These results indicate that, in a first stage, the O<sub>3</sub> slightly develops the porosity of the carbon, increasing its surface area. As the time of exposure lengthens, the pore walls are destroyed by the gasification of the carbon, with a resulting reduction in the surface area. Moreover, the formation of surface oxygen groups at the entrance to the pores may obstruct N<sub>2</sub> access to the micropores.

**3.3. Adsorption Properties. Methylene Blue Adsorption Index.** Methylene blue is widely used to evaluate the adsorption properties of activated carbons.<sup>16</sup> The methylene blue molecule is apolar with a minimum diameter of approximately 0.9 nm, so that it is adsorbed only on micropores of a larger size, mesopores, and macropores.

Table 5 shows the amount of methylene blue adsorbed in the samples,  $X_m(MB)$ . The amount reduces with the length of treatment time, because of the decrease in the surface area of the carbon caused by the ozone treatment. Furthermore, the amount of oxygen chemisorbed on the carbon surface also increases with this treatment (Table 2). This oxygen extracts electrons from the  $\pi$  band of the carbon, reducing the interactions between the methylene blue molecules and carbon. This is due to the weakening

of dispersion forces between the  $\pi$  electron system of the aromatic ring of methylene blue and the  $\pi$  band of the graphitic planes of the carbon, which are finally responsible for the adsorption.<sup>31</sup> Considering the area of the methylene blue molecule<sup>32</sup> to be 1.62 nm<sup>2</sup>, the surface of carbon occupied by this adsorbate ( $S_{MB}$ ) was calculated (Table 5). These values ranged from 328 m<sup>2</sup>/g (sample F) to 256 m<sup>2</sup>/g (sample F-120). In all of the samples, this surface area was greater than the external surface area, indicating that the methylene blue is adsorbed not only on the macropores and mesopores but also on a certain fraction of micropores.

#### 4. Conclusions

The combined utilization of ozone and activated carbon in wastewater treatment leads to the modification of the carbon surface chemical properties and its adsorptive and textural characteristics. The prolonged exposure of activated carbon to ozone gas transforms the chemical composition of the carbon surface. Basic sites are transformed into acid sites because of oxidation. During the treatment, new acid sites are generated, because of the addition of ozone to the double bond of the carbon structure. The extensive oxidation undergone by the carbon generates acid groups, such as anhydride, lactones, and carboxylic acid. The latter group is the main cause of the development of the surface charge. The modification in the oxygenated groups distribution on the carbon surface influences the adsorptive properties of the original carbon. The ozone action also impacts on the carbon textural characteristics; the surface area decreases because of the ozone attack and due to the increase in oxygenated groups prevents the diffusion of the nitrogen, by obstructing the entrances of the micropores. These phenomena also reduce the capacity of the carbon to adsorb methylene blue.

**Acknowledgment.** The authors wish to thank the FONDECYT (Grant Nos. 2000130 and 1010881) for their financial support and Prof. Pedro Toledo and Dr. Nelson Alarcón, of the Surface Analysis Laboratory at the Chemical Engineering Department, University of Concepcion, who conducted the XPS assessment.

LA010920A

(29) Corapcioglu, M. O.; Huang, C. P. *Carbon* **1987**, *25*, 569–578.  
 (30) Barton, S. S.; Evans, M. J. B.; Halliop, E.; MacDonald, J. A. F. *Carbon* **1997**, *35*, 1361–1366.

(31) Radovic, L. R.; Moreno-Castilla, C.; Rivera-Utrilla, J. In *Chemistry and Physics of Carbon*; Radovic, L. R., Ed.; Marcel Dekker: New York, 2000; Vol. 27, p 227.

(32) Graham, D. J. *Phys. Chem.* **1955**, *59*, 896–900.